

Miniature PT Cryocooler Activated by Resonant Piezoelectric Compressor and Passive Warm Expander

S. Sobol, G. Grossman

Technion – Israel Institute of Technology, Haifa, Israel

E-mail: sobols@technion.ac.il

Abstract. A novel type of PZT-based compressor operating at mechanical resonance, suitable for pneumatically-driven Stirling-type cryocoolers, was presented at CEC-ICMC 2015. The detailed concept, analytical model and the test results on the preliminary prototype were reported earlier and presented at ICC17. Despite some mismatch between the impedances and insufficient structural stiffness, this compressor demonstrated the feasibility to drive our miniature Pulse Tube cryocooler MTSa, operating at 103 Hz and requiring an average PV power of 11 W, filling pressure of 40 Bar and a pressure ratio of 1.3. At ICC19 the prototype of a miniature passive warm expander (WE) was presented. The WE mechanism included a phase shifting piston suspended on a silicone diaphragm, a mass element, and a viscous damping system. Several technical drawbacks prevented perfect matching between the WE and MTSa; however, the presented prototype proved the ability to create any flow-to-pressure phase appropriate for a PT cryocooler. This paper concentrates on integration of the MTSa cryocooler with the recently modified PZT compressor operating at corrected mechanical resonance and the modified WE, which was also updated recently to match the MTSa requirements.

1. Introduction

A linear compressor driven by a PZT stack-type actuator, operating at mechanical resonance and suitable for pneumatically-driven Stirling-type cryocoolers, was presented in previous papers [3][4]. The dynamics of the compressor are provided by elastic deformations of the PZT stack, flexural bearings and diaphragms. The only moving part that may be subject to friction and wear is the hydraulic piston; however, it is isolated within the hydraulic volume and thus cannot contaminate the filling gas. It was shown that in case of providing sufficiently high structural stiffness of the dynamic part, the compressor has the potential of effective, high power density and extremely long-time operation.

Detailed modelling, simulations and preliminary tests allowed us to create a functional PZT compressor, suitable for driving our miniature PT cryocoolers of MTS series, which are noted by their 12 mm long regenerators. MTSa equipped by an Inertance Tube (IT) phase shifter showed the best performances, providing 0.4 W of cooling at 110 K, while operating at 103 Hz with filling pressure of 40 Bar and a pressure ratio of 1.3 [2]. The no-load temperature was measured at 99 K. In recent years our research was concentrated mostly on compressors and phase shifters; thereby, for maximum flexibility in experiments with different equipment, a new version of MTSa, called MTSb, was constructed. MTSb is split into maximum number of separate components, which can be easily



replaced and reassembled on demand. However, due to imperfections of the modular assembly, the MTSb reaches a no-load temperature of 105 K and the nominal 0.4 W cooling at about 115 K.

While the demonstrated PZT compressor has been already validated for ability to drive our MTS cryocoolers with the nominal pressure ratio of 1.3 in the range of frequencies 100-120 Hz, the phase shifting mechanism implemented by a passive mechanical Warm Expander (WE) had to be significantly improved for matching the PT requirements [5]. The objectives behind the replacement of the IT system by the mechanical WE were the overall miniaturization and the ability to create a proper flow-to-pressure phase while retaining the required flow amplitude regardless of the PT dimensions and the operating frequency. As shown in [5], the effectiveness of the IT system inherently degrades as the adjoining PT cryocooler is scaled down and/or the operating frequency increases.

2. Passive Warm Expander

Figure 1 demonstrates schematically the proposed warm expander system. The dynamic part of the system consists of two coaxial pistons linked together by a rigid rod, thus producing three gas volumes within the WE housing: front volume (V_f) connected directly to the PT cryocooler, intermediate volume (V_i) and buffer volume (V_b). The corresponding absolute pressures are given by P_f , P_i and P_b , while at static conditions all three are uniform and equal to the filling pressure of the PT cryocooler, P_0 . The secondary piston (A_2) has small apertures filled by porous material, which allow the gas to flow from V_b to V_i and vice versa with some hydraulic resistance, thus producing a damping effect on the axial oscillations.

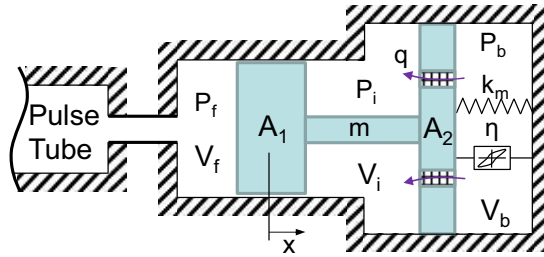


Figure 1. Schematic of the passive warm expander.

The first actual version of the proposed passive WE accompanied by basic calculations and preliminary test results was demonstrated earlier [5]. It was shown that a passive oscillator with the primary piston diameter A_1 suspended on mechanical spring with stiffness k_m should possess the following mass and damping coefficient in order to match the PT requirements:

$$\begin{cases} m = \frac{k_g + k_m}{\omega_0^2} \\ c = \frac{k_g |\tan \theta_0| - \eta k_m}{\omega_0} \end{cases}, \quad -180^\circ < \theta_0 < -90^\circ \quad (1)$$

Where:

$$k_g = \frac{P_{f1} A_1^2 |\cos \theta_0|}{V_{f1}} \quad (2)$$

Regarding (1) and (2): $\omega_0 = 2\pi f_0$, f_0 is the operating frequency; P_{f1} , V_{f1} and θ_0 are the desired pressure amplitude, swept volume amplitude and stroke-to-pressure phase on the A_1 piston front boundary; and η is the hysteresis factor, applicable mostly for elastomeric springs or elastomeric diaphragms. The expressions in (1) were developed assuming the ideal case, where the gas compression in the intermediate and buffer volumes was neglected, and the A_2 piston was subject only to the damping

force. Recently, the linear theory has been modified using fewer assumptions for deeper analysis of the WE system and more accurate predictions.

2.1. Modified Linear Analytical Model

The linear dynamics of the WE system are governed by the following equation:

$$m\ddot{x} + k_m(1 + i\eta)x = (P_f - P_i)A_1 + (P_i - P_b)A_2 \quad (3)$$

Where, x is the displacement of the pistons, $i = \sqrt{-1}$. Relying on [1], the linear mass conservation equations within the intermediate and the buffer volumes can be given by (4) and (5) respectively:

$$-\frac{P_0}{RT_0}q = \frac{V_{b0}\dot{P}_b}{\gamma RT_0} + \frac{P_0\dot{V}_b}{RT_0} \quad (4)$$

$$\frac{P_0}{RT_0}q = \frac{V_{i0}\dot{P}_i}{\gamma RT_0} + \frac{P_0\dot{V}_i}{RT_0} \quad (5)$$

Where, q is the volumetric flow rate through the apertures in piston A_2 , γ is the adiabatic constant, R is the gas constant, and T_0 is the time average temperature. In general, zeros in the subscripts represent time average values of the variables. The volume change rates can be expressed in term of the pistons speed:

$$\begin{aligned} \dot{V}_b &= -A_2\dot{x} \\ \dot{V}_i &= (A_2 - A_1)\dot{x} \end{aligned} \quad (6)$$

The volumetric flow q is supposed to be linearly dependent on the pressure drop on the A_2 piston. The linear flow coefficient is given by C_V :

$$q = -C_V(P_i - P_b) \quad (7)$$

After a substitution of (6) into (4) and (5), a set of four equations with four dependent variables x , q , P_i and P_b is obtained. Assuming pure sinusoidal behaviour of the variables with time, it is convenient to solve the set using phasor transformations. The driving front volume pressure is assumed to have a zero phase:

$$P_f = P_{f1} \cos(\omega t) = \Re(P_{f1}e^{i\omega t}) \quad (8)$$

Solution for x in terms of amplitude x_1 and phase θ is given by (9):

$$\left\{ \begin{aligned} x_1 &= \frac{P_{f1}A_1}{\sqrt{\left(\eta k_m + \omega \frac{c_1 - k_1/\omega_1}{1 + (\omega/\omega_1)^2}\right)^2 + \left(k_m - \omega^2 m + \frac{k_1 + \omega^2 c_1/\omega_1}{1 + (\omega/\omega_1)^2}\right)^2}} \\ \tan \theta &= \frac{\eta k_m + \omega \frac{c_1 - k_1/\omega_1}{1 + (\omega/\omega_1)^2}}{k_m - \omega^2 m + \frac{k_1 + \omega^2 c_1/\omega_1}{1 + (\omega/\omega_1)^2}} \end{aligned} \right. \quad (9)$$

Where:

$$\omega_1 = C_V \gamma P_0 \left(\frac{1}{V_{i0}} + \frac{1}{V_{b0}} \right), \quad k_1 = \frac{\gamma P_0 A_1^2}{V_{i0} + V_{b0}}, \quad c_1 = \frac{(A_2 - A_1)^2 V_{b0} + A_2^2 V_{i0}}{C_V (V_{i0} + V_{b0})} \quad (10)$$

In the modified WE model one can notice the effective viscous coefficient (11), which is frequency dependent, and its value decreases as the operating frequency increases. Furthermore, the model solution provides the expression for the internal gas spring (12), which simplifies to k_l for low frequencies, and increases with the frequency asymptotically up to $\omega_1 c_1$. Both viscous coefficient

reduction and gas stiffness increase are the results of the gas flow q decrease with the frequency. The gas merely has less time to travel from V_b to V_i and vice versa as the frequency increases.

$$c(\omega) = \frac{c_1 - k_1/\omega_1}{1 + (\omega/\omega_1)^2} \quad (11)$$

$$k_{\text{int}}(\omega) = \frac{k_1 + \omega^2 c_1/\omega_1}{1 + (\omega/\omega_1)^2} \quad (12)$$

Combining the results given by (11) and (12) with the equations in (1) allows making a modified prediction of the required WE mass and the flow coefficient for matching the PT requirements at ω_0 . Moreover, ω_0 is generally about two orders of magnitude lower than ω_1 ; therefore, for simplicity, their squared ratio can be neglected relative to unity. The prediction of the required C_V and m for the proposed WE is given by (13):

$$\begin{cases} C_V \approx \frac{\omega_0}{k_g |\tan \theta_0| - \eta k_m} \left(A_2 - \frac{V_{b0}}{V_{i0} + V_{b0}} A_1 \right)^2, & -180^\circ < \theta_0 < -90^\circ \\ m \approx \frac{k_g + k_m + k_1}{\omega_0^2} + \frac{c_1}{\omega_1} \end{cases} \quad (13)$$

2.2. Design

Figure 2 shows a cross section of the proposed WE system accompanied by a list of its major components. Pistons A_1 and A_2 are implemented by piston-diaphragm-cylinder bonded assemblies with effective diameters of 5 mm and 14 mm respectively. The diaphragms were moulded from adhesive fluid silicone of Shore A25. Geometries of the diaphragms were optimized numerically for minimizing the axial stiffness while providing 1.5 mm of travel amplitude and withstanding the operational pressures. Reduction of the stiffnesses and the subsequent k_m is important mostly for miniaturization of the WE system, since it reduces the required moving mass according to equation (13). In fact, the mass dictates the overall dimensions of the WE housing, since it captures most of the interior space. Moreover, the enlarged mass increases the induced vibrations.

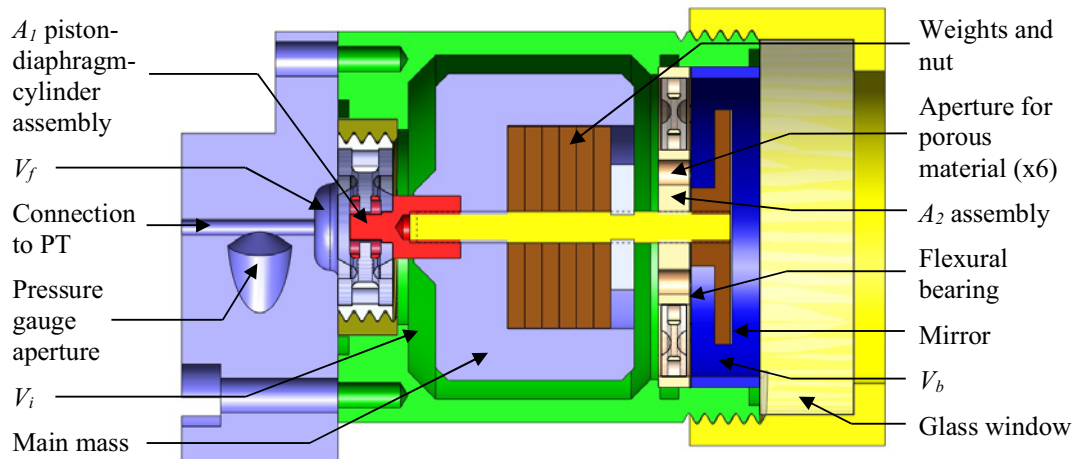


Figure 2. CAD model of the warm expander system.

One of the drawbacks in the previous version of the WE system was the excitement of parasitic motion modes, such as swinging and spinning of the dynamic part. In order to shift the unwanted modes to much higher frequencies it was decided to add a single metal spiral-shape flexural bearing of

very low axial stiffness. The internal rigid area of the flexural bearing is fastened between the A_2 piston assembly and the mirror component. The mirror within the buffer volume together with the glass window provide the ability to measure in real time the displacement of the WE using an external laser-PSD (Position Sensitive Detector) system.

3. Optimization

The PZT compressor was designed to drive our miniature MTSb PT cryocooler operating at 103 Hz, as well as the follow-on models, which should have similar dimensions, but operate at higher frequencies [3]. Since the last report, the compressor has been slightly modified by replacing a polymer diaphragm on the liquid-gas interface by a miniature metallic bellows component. The soft bellows eliminated the gas penetration problem, but had no effect on the short-term performances of the compressor.

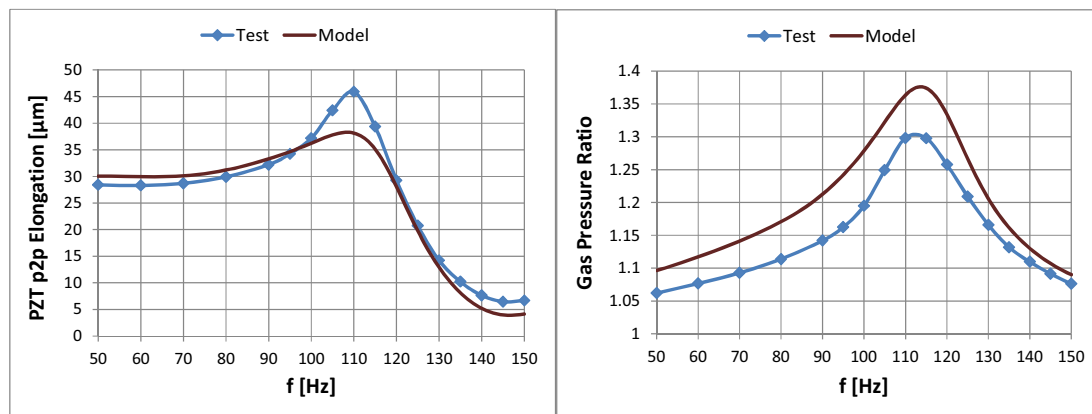


Figure 3. Measured and calculated frequency responses of the PZT compressor [4].

Figure 3 shows some experimental and analytical results on the PZT compressor reported in [4], while being attached to the MTSb cryocooler equipped with the IT phase shifting system [3]. The PZT actuator was driven by a pure sine voltage with peak-to-peak value of 600 V, which is 60% of the maximum allowable voltage for this type of actuator. According to Figure 3 the PZT actuator develops the maximum amplitude at a frequency 110 Hz, whereas the maximum electro-mechanical conversion factor is obtained at about 115-120 Hz. These frequencies mismatch the MTSb optimum; however, the cryocooler performances are less sensitive to the operating frequency as long as a phase shifting mechanism provides the proper flow conditions at the hot end. Therefore, it was decided to optimize the new WE for operation at 110 Hz as a compromise, thus adapting the new working point to both the PZT compressor and the cryocooler preferences.

One of the main challenges in the WE design was the reduction of the axial mechanical stiffness k_m , originated from elasticity of both diaphragms and the metallic flexural bearing. The final WE diaphragms together with the compressing diaphragm of the PZT compressor are shown in Figure 4. The total value of k_m was measured at 7.0 N/mm, which is almost twice lower than the stiffness obtained in the previous version of the WE.

According to the SAGE™ model the WE with the piston diameter of 5 mm, connected by a 20 mm long transfer line with ID 0.7 mm, should provide the travel amplitude of 1.36 mm and the stroke-to-pressure phase of -150° . Pressure amplitude on the A_1 front boundary is estimated at 4.4 bar while the pressure amplitude within the aftercooler is retained at 5.2 bar, which is equivalent to the pressure ratio of 1.3. From equation (2) the front gas stiffness k_g is estimated then at 5.5 N/mm. The hysteresis factor η of the employed silicone rubber was estimated in the previous work at about 0.1. The WE housing intermediate and buffer void volumes are 2.0 cc and 1.2 cc respectively. According to

equation (13), for operation at 110 Hz, the required flow coefficient C_V and the required oscillating mass m are estimated at 5.99×10^{-9} (m³/s)/Pa and 27.9 gr respectively.

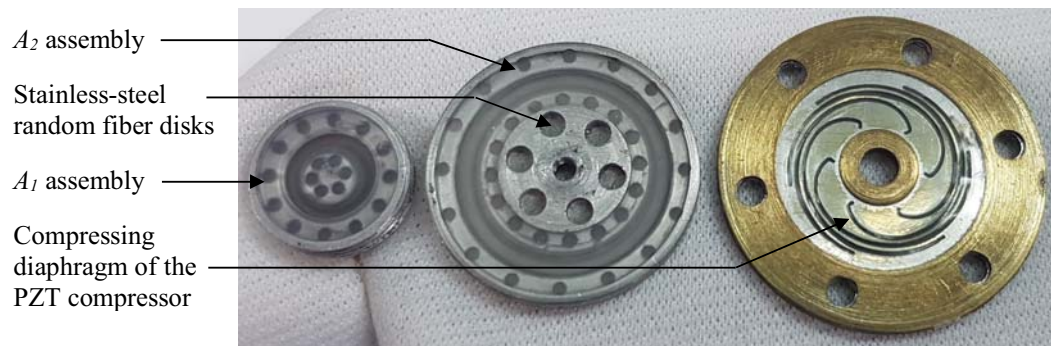


Figure 4. Diaphragms employed in the PZT- driven MTSb cryocooler equipped with the WE.

4. Experiment setup

Performances of the PZT compressor and the WE system were investigated while being connected to our MTSb miniature PT cryocooler. Due to the modular structure of the cryocooler and the mounting structure, it was quite easy to replace the PZT compressor by the conventional one, or the IT system by the WE and vice versa, thus enabling comparisons between the respective performances. Figure 5 shows pictures of the PT assembly with different phase shifters and the appropriate measurement equipment. Void volume of the reservoir shown on the left picture is 10 cc, while the external reservoir dimensions capture volume of about 45 cc due to the increased wall thickness. The vacuum chamber encloses the presented assemblies by covering and fastening to the mounting plate. The compressor is mounted on the opposite side of the plate, outside the vacuum chamber.

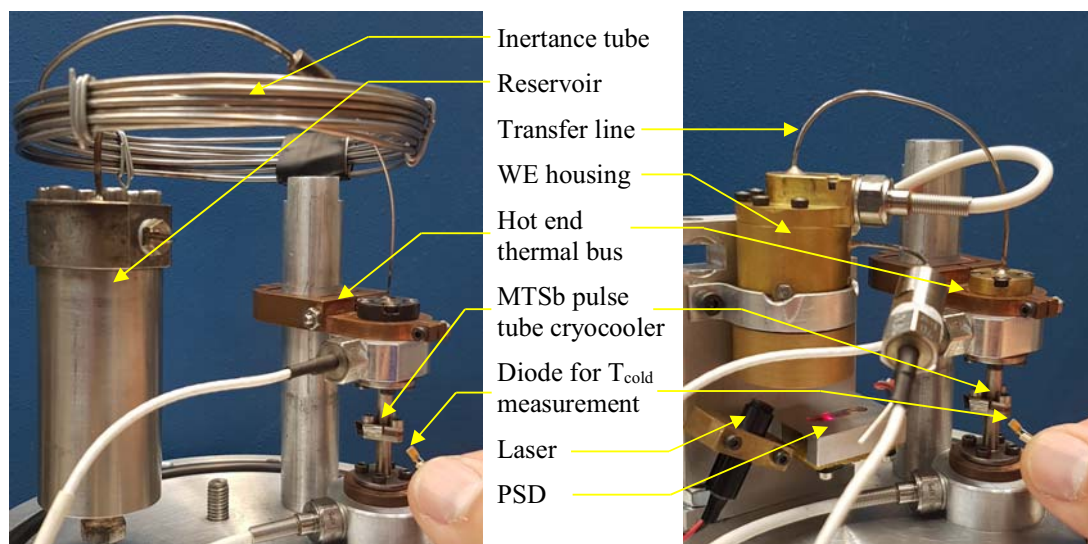


Figure 5. MTSb PT cryocooler equipped with IT (on left) and WE (on right) phase shifters.

Since the main purpose of experiments was studying of the WE functionality compared to the IT system, there was no need to wrap the PT cold end by Mylar, thus reducing the radiation heat transfer. In any case, the cool-down was not started before the pressure within the vacuum chamber dropped below 10^{-4} Torr. During the experiments the cold end temperature was measured by a miniature diode-type sensor, having accuracy of 0.1 K. Temperatures of the hot heat exchangers were measured by K-

type thermocouple, since the accuracy is not as critical in this case. Miniature fast pressure gauges were installed on both hot sides of the PT cryocooler, on both sides of the A_1 piston within the WE housing and within the liquid volume of the PZT compressor. All the pressures, strain gauges attached to the PZT actuator and the laser-PSD system intended for the WE were sampled synchronically at a frequency of 20 kHz per channel and recorded on demand.

5. Results

Figure 6 shows the ultimate cool-down curves of the MTSb cryocooler equipped with the IT and the WE phase shifting systems, while the experiments were conducted in vacuum, but with no use of the radiation shield. In the case of the IT, the lowest measured temperature at the cold end was 110.1 K, and it was obtained at 103 Hz. With the WE system we succeeded to attain 108.7 K at 113 Hz. In both cases the filling pressure was 40 bar, and the pressure ratio within the after-cooler was retained at 1.3 during all the experiment. The cool-down process of MTSb with the IT took about two minutes, while with the WE the period was about 10 seconds shorter, most probably due to the higher operating frequency.

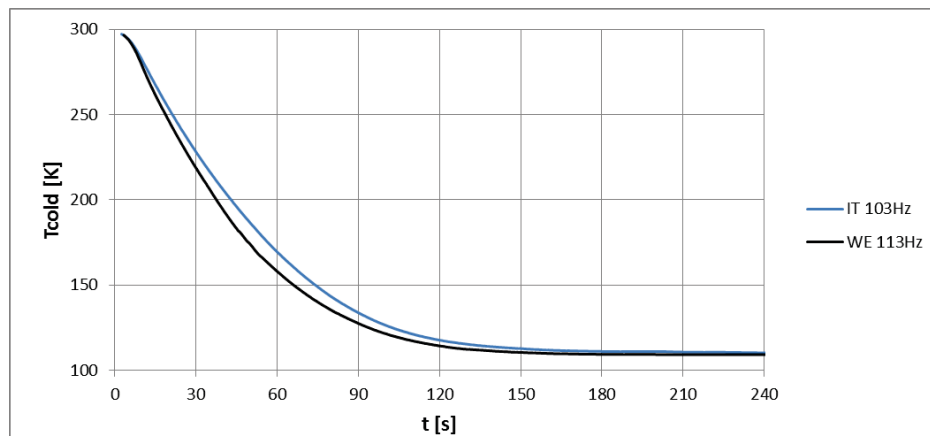


Figure 6. Cooling-down of MTSb cryocooler with IT and WE phase shifting systems.

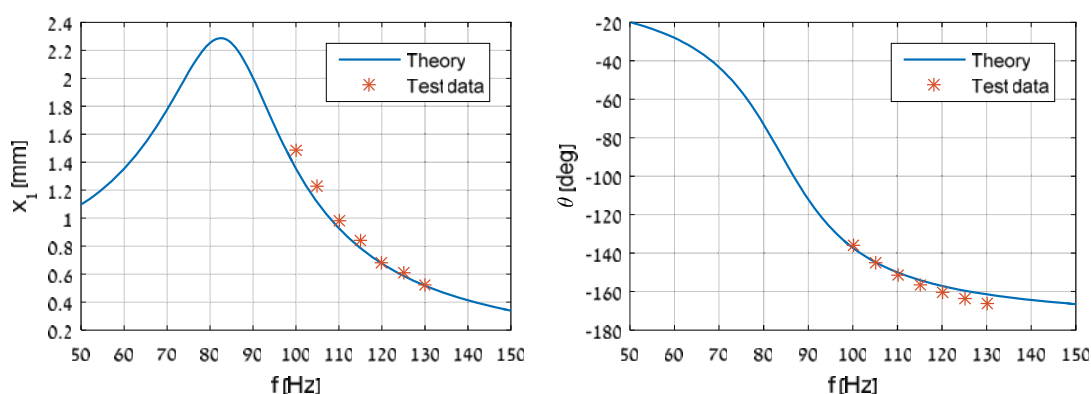


Figure 7. Measured frequency response of the WE versus the theoretical model for $P_{fi} = 3$ bar.

The lowest cold end temperature of the MTSb cryocooler equipped with the WE system was attained while the oscillating mass was 30 gr, and the flow coefficient was estimated experimentally at about 7.0×10^{-9} (m³/s)/Pa. At 113 Hz and nominal pressure ratio the measured travel amplitude of the WE was about 1.4 mm and the stroke-to-pressure phase was estimated at -155° . These values are very

close to those predicted by the SAGE model; however, the parameters m , C_r , and the optimum operating frequency slightly differ from those predicted analytically. Nevertheless, from the comparison of the frequency responses shown in Figure 7, one can notice that the theoretical curves based on the optimum analytical solution parameters and the test data obtained from the trial and error optimization demonstrate quite a good matching.

6. Conclusions

A miniature PT cryocooler was successfully integrated with a resonant piezoelectric compressor and the recently developed passive warm expander at 113 Hz. This frequency allowed the PZT compressor to operate efficiently, while the cryocooler did not show signs of performance degradation despite a design frequency of 100 Hz. The main achievement in this work was the successful redesign of the passive WE system for matching the PT requirements. Eventually, the WE was capable of providing a sufficient flow-to-pressure phase shift and the proper travel amplitude resulting in improved cold end temperature of the cryocooler relative to the one obtained with the IT system.

Because of the need to mount the measurement equipment, the external dimensions of the WE housing were set at 45×Ø28 mm; without this equipment the dimensions may be easily reduced to 33×Ø25 mm. In any case, the WE structure is more compact relative to the IT-reservoir assembly, mostly because of the absence of the inertance tube. Furthermore, for any similar PT cryocoolers designed to operate at higher frequencies, the required oscillating mass will decrease, resulting in further miniaturization of the WE housing. This trend would be realized in the future works, thus to close the gap between the sizes of the main pulse tube components and the phase shifter.

A modified linear model developed for the passive WE with pneumatic damping system was successfully validated and determined to be useful for the initial estimation of the WE parameters. The actual physics is more complicated due to the non-linearities of the gas springs, of the diaphragms' stiffness and of the gas flow restrictions. Therefore, additional trial-and-error optimization of parameters is required for the fine tuning of the WE performance. In our case the lowest cold end temperature was achieved at 113 Hz instead of 110 Hz, while the oscillating mass was set to 30 gr instead of the predicted 27.9 gr, and the flow coefficient of the damping system was 7.0×10^{-9} instead of 6.0×10^{-9} (m³/s)/Pa. Other WE parameters were the same for the actual assembly and the analytical model.

Acknowledgment

The generous financial help of the Rechler Family, MAFAT and the Technion is gratefully acknowledged.

References

- [1] Radebaugh R., 1990: A Review of Pulse Tube Refrigeration. *Advances in Cryogenic Engineering*, **35**, pp 1191-1205.
- [2] Sobol S., Katz Y. and Grossman G., 2010: A study of a miniature in-line pulse tube cryocooler. *International Cryocooler Conference*, **16**, pp 87-95.
- [3] Sobol S., Sofer T. and Grossman G., 2012: Development of a linear compressor for Stirling-type cryocoolers activated by piezoelectric elements in resonance. *International Cryocooler Conference*, **17**, pp 331-340
- [4] Sobol S. and Grossman G., 2015: Linear resonance compressor for Stirling-type cryocoolers activated by piezoelectric stack-type elements. *IOP Conf. Series: Materials Science and Engineering*, **101**, 012093/1-9.
- [5] Sobol S., and Grossman G., 2016: Diaphragm-type mechanism for passive phase shifting in miniature PT cryocooler. *International Cryocooler Conference*, **19**, pp 219-228.